Journal of Physics: Condensed Matter

The *p–T* phase diagram of ammonium hexafluoroaluminate

INSTITUTE OF PHYSICS PUBLISHING JOURNAL OF PHYSICS: CONDENSED MATTER

J. Phys.: Condens. Matter **14** (2002) 6447–6453 PII: S0953-8984(02)35115-4

The p–T phase diagram of ammonium hexafluoroaluminate

M V Gorev[1], I N Flerov[1], A Tressaud[2] and E Durand[2]

[1] L V Kirensky Institute of Physics, 660036 Krasnoyarsk, Russia
[2] Institut de Chimie de la Matière Condensée de Bordeaux, 33608 Pessac, France

E-mail: gorev@iph.krasn.ru and tressaud@icmcb.u-bordeaux.fr

Received 21 March 2002
Published 14 June 2002
Online at stacks.iop.org/JPhysCM/14/6447

Abstract

The heat capacity and the effect of hydrostatic pressure on structural phase transitions in ammonium hexafluoroaluminate, $(NH_4)_3AlF_6$, have been studied. Two heat capacity anomalies have been found with maxima at $T_1 = 218.5 \pm 0.5$ K and $T_2 = 179 \pm 2$ K. Respective entropy changes of phase transitions are $\Delta S_1 = 15.3 \pm 0.5$ J mol^{-1} K^{-1} and $\Delta S_2 = 2.5 \pm 0.5$ J mol^{-1} K^{-1}. It is shown that the p–T phase diagram of this compound is rather complex and contains a triple point ($p_{tp} = 0.12$ GPa, $T_{tp} = 221$ K) and high-pressure phase. The mechanism of transformations and generalized p–T phase diagram for compounds of the $(NH_4)_3M^{III}F_6$ family are discussed within the framework of the rotational order–disorder model.

1. Introduction

Phase transitions in hexafluorometallates(III) of elpasolite and cryolite families, $A^I_2B^IM^{III}F_6$ and $A^I_3M^{III}F_6$, are of great interest because these series provide varied sequences of group-to-subgroup family trees. Single or successive phase transitions are observed when lowering temperature from the high-temperature prototype, which is derived from the perovskite structure with an $Fm\bar{3}m$ symmetry. Both temperatures and sequences of phase transitions are very sensitive to the external pressure and to the size of M^{3+} ions.

$(NH_4)_3M^{III}F_6$ cryolite compounds containing small trivalent ions such as Cr^{3+}, Fe^{3+} and Ga^{3+} generally exhibit only one phase transition, directly from $Fm\bar{3}m$ symmetry to $P\bar{1}$ triclinic symmetry [1–4], whereas the presence in the structure of large M^{3+} ions leads to a succession of three phase transitions with two intermediate monoclinic phases [5–7]. Recent investigations of the pressure–temperature (p–T) phase diagram of these systems [6] have demonstrated that the two intermediate monoclinic phases observed at atmospheric pressure in ammonium cryolites with large M^{3+} ions disappear at higher pressures and a straightforward $Fm\bar{3}m \rightarrow P\bar{1}$ phase transition is thus observed, as in the case of compounds with smaller M^{3+} ions at atmospheric

0953-8984/02/256447+07$30.00

pressure. On the other hand, in $(NH_4)_3GaF_6$, the effect of pressure leads in a first step to a sequence of two phase transitions at the first triple point (0.045 GPa) and then to a triple point at 0.25 GPa [6]. The compound $(NH_4)_3AlF_6$, which has the smallest unit-cell volume among the cubic ammonium cryolites, undergoes at room pressure one [8, 9] or two [10, 11] phase transitions according to different authors. Changes in the sequence of phase transitions can be expected under pressure.

In this paper we reinvestigate the calorimetric study of $(NH_4)_3AlF_6$ at room pressure and determine the effect of hydrostatic pressure on structural phase transitions. A generalized p–T phase diagram is proposed for the ammonium cryolite family.

2. Experimental methods and results

2.1. Sample preparation and x-ray characterization

$(NH_4)_3AlF_6$ cryolite was prepared using solid-state reaction. This reaction was carried out in a platinum tube sealed under inert atmosphere, using a stoichiometric mixture of NH_4F and the metal trifluoride AlF_3. The mixture had been previously ground in a glove box under Ar because of the hygroscopicity of the starting compounds. The reaction conditions, several tens of hours at 300 °C, were reached after a gradual increase in temperature.

The structural characterization of the compound was performed using x-ray powder diffractometry, the sample being set in an air-tight cell with a Mylar window. No additional phases were found. The unit-cell constant $a_0 = 8.937(1)$ Å was calculated after a refinement of the spectrum at room temperature in the cubic $Fm\overline{3}m$ ($Z = 4$) space group.

2.2. DSC measurements

Calorimetric measurements were carried out with a Perkin–Elmer DSC-7 differential scanning calorimeter working down to 100 K. The compound was sealed in an aluminium sample holder. Temperatures and enthalpy were calibrated using two samples: the melting temperature of pure indium and the melting temperature of pure mercury. The temperatures were determined with accuracy of ±0.2 K and the uncertainty on the enthalpy value was estimated as ±5 J mol^{-1}. The experiments were carried out in a He gas atmosphere. The heating and cooling rates were fixed at 5 K min^{-1}.

The temperature dependences of heat capacity on cooling and heating are shown in figure 1. Two heat capacity anomalies were found with maxima at $T_1 = 218.5 \pm 0.5$ K and $T_2 = 179 \pm 2$ K. Both phase transitions are first-order transformations with thermal hysteresis $\delta T_1 = 2.5$ K and $\delta T_2 \approx 25$ K. The temperatures T_1 and T_2 are different from the phase transition temperatures reported previously: 220.8 and 193 K [11]. The largest difference (∼14 K) is observed for the temperature of the second phase transition and may be due to the peculiar features of this transformation and to different preparation methods: synthesis techniques based on fluoride aqueous solutions were used in [11]. It can be added that dielectric and thermocurrent measurements have shown that a maximum of permittivity was observed close to T_1, with the occurrence of a residual polarization below T_1 [12].

The dotted curve in the transition region (figure 1) represents the normal heat capacity estimated by smoothed interpolation of the heat capacity data above and below phase transitions by combination of Debye's and Einstein's functions. The entropy changes at transitions based on the excess heat capacity were estimated as $\Delta S_1 = 15.3 \pm 0.5$ J mol^{-1} K^{-1} and $\Delta S_2 = 2.5 \pm 0.5$ J mol^{-1} K^{-1}. These values are less than corresponding ones determined by adiabatic calorimetry [11]. It is necessary to point out that DSC provides reliable information

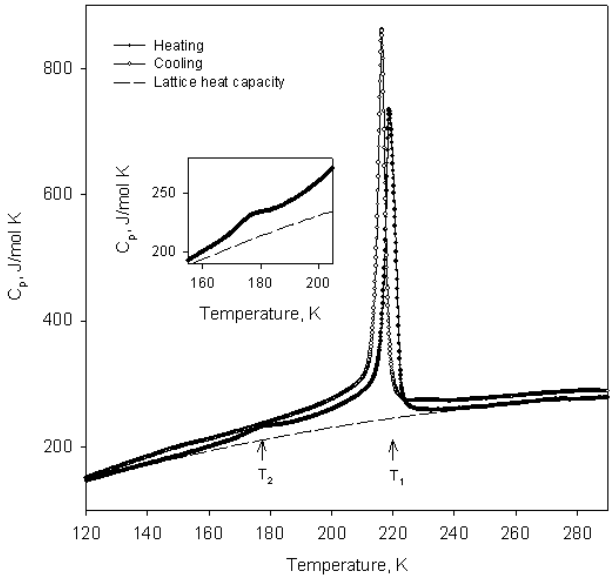

Figure 1. Heat capacity of $(NH_4)_3AlF_6$ measured by DSC on heating and cooling. The inset shows the results near the $G_1 \rightarrow G_2$ phase transition on heating.

about entropy change when the phase transition is a first-order one distant from a tricritical point. The results are more accurate if the entropy jump at the transition temperature is the majority of the total entropy change. In Al cryolite the heat capacity exhibits a long tail toward lower temperatures, which indicates the closeness of the transformations to tricritical points and hinders an accurate extraction of the full anomalous part of the heat capacity and thus ΔS determination.

2.3. DTA under pressure

The effect of hydrostatic pressure was studied on the powdered samples which had been previously used for calorimetric measurements. The variation of phase transition temperatures was measured by means of differential thermal analysis (DTA). Pressure up to 0.6 GPa was generated in a DTA vessel of piston-and-cylinder type associated with the multiplier. Silicon oil was used as the pressure-transmitting fluid. Owing to its high sensitivity, a germanium–copper thermocouple was utilized as a differential device. Quartz as a reference substance and a small copper container ($\sim$0.05 cm^3) filled with powdered sample were fixed with glue onto two thermocouple junctions. Pressure and temperature were measured with a manganin gauge and copper–constantan thermocouple with an accuracy of about $\pm 10^{-3}$ GPa and ± 0.3 K, respectively.

The p–T phase diagram of $(NH_4)_3AlF_6$ is shown in figure 2. The notation for the distorted phases is the same as for the generalized phase diagram proposed in figure 3. At room pressure two DTA anomalies were registered, which correspond to $G_0 \rightarrow G_5$ and $G_5 \rightarrow G_3$ phase transitions. Both transition temperatures decrease with increasing pressure. The former transition splits at the triple point ($p_{tp} = 0.12$ GPa, $T_{tp} = 221$ K) into a sequence of two transformations, $G_0 \rightarrow G_4 \rightarrow G_5$. Because of the smearing and very rapid intensity decrease of $G_0 \rightarrow G_5$ and $G_4 \rightarrow G_5$ with pressure, the DTA anomalies associated with these phase transitions could only be detected in a narrow pressure range. All phase boundaries are almost

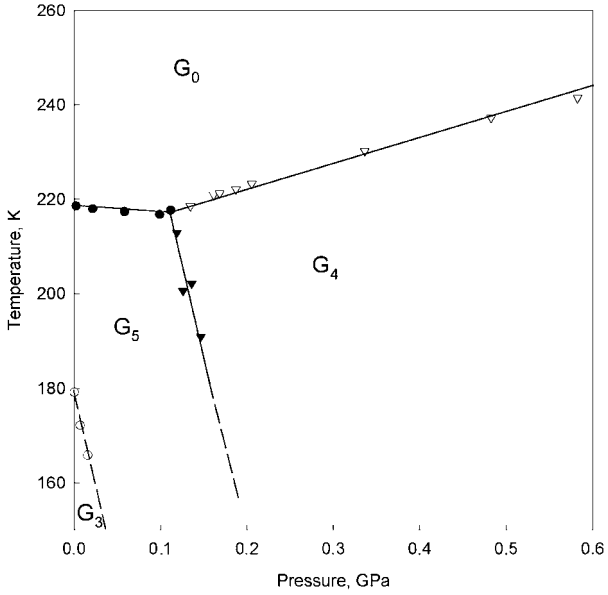

Figure 2. p–T phase diagram of $(NH_4)_3AlF_6$.

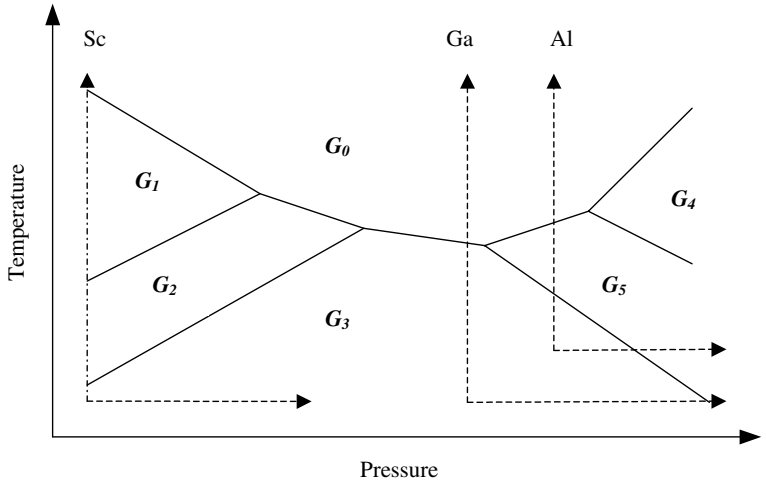

Figure 3. Generalized p–T phase diagram of the $(NH_4)_3M^{III}F_6$ family. Dashed lines correspond to the phase transition sequences at $p = 0$ for Sc, Ga and Al cryolites, respectively.

linear. The corresponding pressure coefficients dT/dp are presented in table 1 together with the values obtained for other ammonium cryolites [6, 12].

The very large dT/dp value for the $G_5 \rightarrow G_3$ transition and the rather small pressure of the triple point could be considered as probable reasons for the discrepancy in the number and temperatures of phase transitions in the previous publications.

Table 1. Thermodynamic parameters of phase transitions in $(NH_4)_3M^{III}F_6$ cryolites (dT/dp in K GPa^{-1}).

		Al	V	Fe	Ga	$Ga_{0.6}Sc_{0.4}$	$Ga_{0.4}Sc_{0.6}$	Sc
$G_0 \rightarrow G_1$	$\Delta S/R$							1.63
	dT/dp						−8.2	−16.4
$G_1 \rightarrow G_2$	$\Delta S/R$							0.81
	dT/dp						46.4	57.5
$G_2 \rightarrow G_3$	$\Delta S/R$							0.08
	dT/dp						65.2	59.9
$G_0 \rightarrow G_3$	$\Delta S/R$		2.99	2.77	2.76	2.60		
	dT/dp				−12.1	−15.3	−8.1	
$G_0 \rightarrow G_4$	$\Delta S/R$							
	dT/dp	50.4 ± 1.2			101.3			
$G_4 \rightarrow G_5$	$\Delta S/R$							
	dT/dp	−670 ± 100			∼0			
$G_5 \rightarrow G_3$	$\Delta S/R$	0.5 ± 0.1						
	dT/dp	−700 ± 100			−22.5			
$G_0 \rightarrow G_5$	$\Delta S/R$	2.22 ± 0.08						
	dT/dp	−11.8 ± 4			73.1	60.1		
Reference		[11] and this work	[1]	[11]	[6]	[13]	[13]	[6]

3. Discussion

As one can see in table 1, the structural transformations in cryolites are followed by rather large values of entropy changes characteristic of order–disorder phase transitions. Starting from structural aspects, NMR and calorimetric data, a model of structural distortions was proposed, which was associated with orientational ordering of fluorine octahedra and ammonium tetrahedra [3, 5, 6, 11].

In $(NH_4)_3MF_6$ phases with $Fm\bar{3}m$ symmetry, $[MF_6]$ and $[(NH_4)F_6]$ octahedra alternate along the three fourfold axes and are linked to each other by common F atoms located at the octahedron vertices. In the assumption that fluorine octahedra behave as rigid structural units, the orientational disorder in the cubic phase was considered to be connected to the presence of fluorine atoms either in 96j or in 192l sites, with an occupancy factor of either 1/4 or 1/8. The choice of 192l sites for F atoms is supported by the good agreement between observed and calculated entropy changes. This result has been recently corroborated by x-ray measurements on an $(NH_4)_3GaF_6$ single crystal [14]. Moreover Raman studies on some ammonium cryolites have confirmed the rigidity of octahedra and tetrahedra, at least in the cubic and monoclinic phases [15].

When ammonium ions occupy two cationic sites, i.e. 8c (CN = 12) and 4b (CN = 6), NH_4 groups have two distinct orientations in the latter case only, in connection with the T_d symmetry of an NH_4 tetrahedron within an O_h site. These two orientations are related to one another by a 90° rotation. It has been shown that ammonium ions in CN = 12 tend to stabilize the structure because their environment is formed by four clusters of F atoms that belong to different (MF_6) groups and that form a regular tetrahedron around (NH_4) entity [3, 11]. Thus the total entropy connected with the structural phase transitions due to the ionic ordering process could be given as the sum of contributions from $[MF_6]$ groups and from the ammonium groups: $\Sigma\Delta S = R(\ln 8 + \ln 2) = 2.77R$. The total entropy change found experimentally for ammonium-based cryolites agrees fairly well with this value within the experimental errors. However, it can be pointed out that in Sc and Al compounds an overlapping of excess

heat capacities occurs between the two successive phase transitions, as shown in figure 1 for $(NH_4)_3AlF_6$. In these conditions, it appears difficult to determine accurately the entropy changes for each transformation separately. One can guess that ammonium ions with CN = 12 are 'passive' structural units, which do not take part in the mechanism of structural distortions because of their ordering in the cubic phase.

The appearance of different phase sequences when applying pressure and temperature are due to interactions which mostly depend on the interatomic distances. The value of unit-cell volume, or the size of the M^{3+} ion, can account for these interactions. The effect of pressure corresponds to a decrease of the volume, and in such conditions the compound may exhibit a behaviour similar to that found at lower pressures for another cryolite with a smaller initial volume, so combining individual p–T phase diagrams and phase transition entropies for different cryolites one can build a generalized phase diagram for the whole family. The generalized phase diagram, which includes all experimental data observed for $(NH_4)_3M^{III}F_6$ cryolites, is proposed in figure 3.

Compounds with large trivalent ions (M^{3+}: Sc, In) exhibit at ambient pressure a succession of three phase transitions $G_0 \rightarrow G_1 \rightarrow G_2 \rightarrow G_3$ with two intermediate monoclinic phases, $G_1 = C_{2h}^5(P12_1/n1, Z = 2)$ and $G_2 = C_{2h}^3(I12/m1, Z = 16)$, and a triclinic low-temperature phase, $G_3 = C_i^1(P\bar{1}, Z = 16)$ [5–7]. Only phase transitions $G_0 \rightarrow G_1$ and $G_1 \rightarrow G_2$ can be associated with the ordering processes according to their entropy values, which are close to $R \ln 8$ and $R \ln 2$, respectively.

From the temperature behaviour of the spin–lattice relaxation time of fluorine atoms and protons in $(NH_4)_3InF_6$ it follows that both $[MF_6]$ and $[(NH_4)F_6]$ 'critical' groups take part in the mechanism of phase transition sequences observed starting from the cubic phase [16]. Therefore in accordance with the $G_0 \rightarrow G_1$ entropy value ($R \ln 8$), in the G_1 phase the ammonium tetrahedra ($4b$) are completely ordered ($R \ln 2$), and the octahedra are partially ordered ($R \ln 4$). The second phase transition can be assigned to the final ordering of the octahedral. This assumption is supported by NMR experiments that show that at this temperature only the behaviour of fluorine is anomalous [16].

The third transition is characterized by a small entropy change. It can be supposed that both phases G_2 and G_3 are completely ordered variants of the initial cubic phase G_0 and differ from each other by the arrangement of the tetrahedron sublattice. Additional structural information is needed to obtain reliable information about the mechanism of this phase transition.

The $G_0 \rightarrow G_1$ transition temperature decreases while the temperatures of $G_1 \rightarrow G_2$ and $G_2 \rightarrow G_3$ transitions increase with increasing pressure (or decreasing M^{3+} ion size). As a result, the temperature regions of phases G_1 and G_2 are narrowed and disappear at triple points ($p_{tp1} = 0.52$ GPa and $p_{tp2} \approx 1.2$ GPa for $(NH_4)_3ScF_6$; $p_{tp1} = 0.22$ GPa and $p_{tp2} \approx 0.38$ GPa for $(NH_4)_3Ga_{0.4}Sc_{0.6}F_6$) [13].

For higher pressures an unique phase transition, $G_0 \rightarrow G_3$, i.e. $Fm\bar{3}m \rightarrow P\bar{1}$, is observed [5]. The triclinic phase is characterized by simultaneous complete ordering of ammonium tetrahedra and fluorine octahedra with a respective entropy change close to the theoretical value: $\Delta S = R(\ln 8 + \ln 2)$. This behaviour is consistent with that observed at $p = 0$ for compounds with smaller M^{3+} cations: Ga, Cr, V and Fe.

A further increase of pressure, which is similar to a decrease in the M^{3+} ion size, leads first to a splitting into a succession of two transitions, $G_0 \rightarrow G_5 \rightarrow G_3$ (occurring at $p > 0.3$ GPa for $(NH_4)_3Ga_{0.6}Sc_{0.4}F_6$ and at $p > 0.05$ GPa for $(NH_4)_3GaF_6$), and then to three structural transformations, $G_0 \rightarrow G_4 \rightarrow G_5 \rightarrow G_3$ (occurring at $p > 0.25$ GPa for $(NH_4)_3GaF_6$ and at $p > 0.12$ GPa for $(NH_4)_3AlF_6$) [13].

Unfortunately, no structural data on G_4 and G_5 distorted phases are available, so far. On the basis of heat capacity measurements we can suppose only that the $G_0 \rightarrow G_5$ phase

transition is associated with the ordering of ammonium tetrahedra ($R \ln 2$) and partial ordering of octahedra ($R \ln 4$), the $G_5 \rightarrow G_3$ transformation being probably connected with a final ordering of the octahedra.

The analysis of the distortion of the cubic prototype structure using the rigid (MF_6) octahedron model has shown that different monoclinic distortions of cryolite structure can be obtained with two possible orientations of octahedra similar to distortions ($0\phi\phi$) and ($0\psi\psi$) in elpasolites with monatomic cations [17]. This point can be considered as the possible reason for different phase sequences ($G_0 \rightarrow G_1 \rightarrow G_2 \rightarrow G_3$ for low pressure and large M^{3+} cations, and $G_0 \rightarrow G_4 \rightarrow G_5 \rightarrow G_3$ for high pressure and small M^{3+} cations) and of the opposite sign of the dT/dp value for $G_0 \rightarrow G_1$ and for $G_0 \rightarrow G_5$ and $G_0 \rightarrow G_4$ phase boundaries.

Additional information about coordinates and thermal parameters of fluorine atoms and protons in both cubic and distorted phases are required to ensure the reliability of the proposed hypotheses. The modification of the orientational motions through the phase transition processes should also be evidenced. For this purpose, deuterated compounds are now in preparation to perform neutron diffraction measurements.

Acknowledgments

This work was supported in part by INTAS (grant 97-10177) and by the Russian Foundation for Basic Research (grant 00-02-16034). The authors are grateful to Dr A D Vasiliev and Professor M Couzi for forwarding unpublished results.

References

[1] Kobayashi K, Matsuo T and Suga H 1985 *Solid State Commun.* **53** 719
[2] Morup S and Thrane N 1972 *Solid State Commun.* **11** 1319
[3] Moriya K, Matsuo T, Suga H and Seki S 1977 *Bull. Chem. Soc. Japan* **50** 1920
[4] Epple M 1978 *Thesis* University of Tübingen
[5] Tressaud A, Khairoun S, Rabardel L, Kobayashi K, Matsuo T and Suga H 1986 *Phys. Status Solidi* a **96** 407
[6] Gorev M V, Flerov I N and Tressaud A 1999 *J. Phys.: Condens. Matter* **11** 7493
[7] Melnikova S V, Misyul S V, Bovina A F and Afanasyev M L 2000 *Fiz. Tverd. Tela* **42** 336 (in Russian)
[8] Vecher R A, Volodkovich L M, Petrov G S and Vecher A A 1985 *Thermochim. Acta* **87** 377
[9] Steward E G and Rooksby H P 1953 *Acta Crystallogr.* **6** 49
[10] Hirokawa K and Furukawa Y 1988 *J. Phys. Chem. Solids* **49** 1047
[11] Moriya K, Matsuo T, Suga H and Seki S 1979 *Bull. Chem. Soc. Japan* **52** 3152
[12] Lorient M, Von der Mühll R, Tressaud A and Ravez J 1981 *Solid State Commun.* **40** 847
[13] Gorev M V, Flerov I N, Tressaud A, Denux D and Fokina V D 2002 *Fiz. Tverd. Tela* **44** at press (in Russian)
[14] Vasiliev A D 2001 private communication
[15] Couzi M 1998 private communication
[16] Sasaki A, Furukawa Y and Nakamura D 1989 *Ber. Bunsenges. Phys. Chem.* **93** 1142
[17] Flerov I N, Gorev M V, Aleksandrov K S, Tressaud A, Grannec J and Couzi M 1998 *Mater. Sci. Eng.* R **24** 81